DOE/NV/25946--488

Lunar Wireless Power Transfer
Feasibility Study

March 2008

Prof. Zoya Popovic, *University of Colorado, Boulder*

David R. Beckett, Scott R. Anderson, Diana Mann, Stuart Walker, *Independent Consultants*

Sheldon Fried, Ph.D., *National Security Technologies, LLC*

Abstract – **This study examines the feasibility of a multi-kilowatt wireless radio frequency (RF) power system to transfer power between lunar base facilities. Initial analyses, show that wireless power transfer (WPT) systems can be more efficient and less expensive than traditional wired approaches for certain lunar and terrestrial applications. The study includes evaluations of the fundamental limitations of lunar WPT systems, the interrelationships of possible operational parameters, and a baseline design approach for a notional system that could be used in the near future to power remote facilities at a lunar base. Our notional system includes state-of-the-art photovoltaics (PVs), high-efficiency microwave transmitters, low-mass large-aperture high-power transmit antennas, high-efficiency large-area rectenna receiving arrays, and reconfigurable DC combining circuitry.**

I. Summary

NASA has embarked on a bold mission to return to the moon and establish a permanent presence. A moon base will require a vast amount of resources that can be extracted from various locations. A key question is how to deliver power to facilities (load stations) distributed on the lunar service, possibly in places where there is little sunlight. Initially, the load stations are planned to be 0.5 to 2km away from mountain-tops where photovoltaic generation stations can be placed. Each site is expected to require 10kW of power to operate.

Traditional power transfer methods for this type of off-site extraction mission would utilize cables, estimated to have a mass of about 7,500kg for five load stations. These transmission lines must traverse large distances, are sensitive to temperature, will be expensive to transport from Earth to the moon, may be a safety hazard for lunar operations, are susceptible to solar flare induced transient effects, have large diameters due to high voltages and power levels, have a large mass, and are difficult to manage due to residual cable stresses.

In addition, once the cables are set up, they would be difficult to move in the event that a different facility needs to be powered. Since multi-kilowatt power requirements are envisioned for these work sites, new methods of power transfer must be explored.

For comparison purposes, a top-level system design for a traditional transmission line approach was developed. A transmission voltage of 480 V was selected based upon minimum cable sizes

and voltage ranges available directly from series/parallel combined solar cells. Higher voltages are possible but conversion losses, insulation requirements, and other inefficiencies become driving factors. For five 10 kW load stations located 2 km away from two generation stations, the following power transmission link system parameters are calculated and compared to corresponding parameters for a traditional transmission line approach (Table 1).

Table 1. Traditional transmission line system parameters compared to WPT system parameters.

Power System Elements	Transmission Line	WPT System	Comments:
Transmission Line Voltage	480 Volts	N/A	User voltage less losses will be down converted to 120 V
Transmission Line Voltage Drop	80 Volts	N/A	Stranded AL Cable with connection losses at nominal 20 degrees C
Temperature Related Voltage Drop	33 Volts	N/A	Lunar Temp = 121 degrees C
Current between Load and Generation Station	21 Amps	N/A	
System mass	7500 kg 500 kg (IC)	4200 kg 50 kg (SA)	Four generation stations with three load stations each, No. 2 Duplex (Plus and Return) cables, Added 25% for packaging and deployment hardware. Additional 500Kg for cable interconnecting (IC) hardware.
Voltage Down Converter	500 kg	500 kg	Mass Est., five Load Stations
Power Transfer Tower	N/A	400 kg	Mass Est., Four generation stations Est. $100K per tower
Power Transfer Efficiency	~60 %	~45 %	
Power Transmission Loss	2,400 W	5,500 W	38.8 m^2 (33 kg) of additional solar array (SA) area required for WPT system, Additional cost = $3.9M
Power Transfer System Cost	$50 K $5 M	$13 M $4 M (SA) $0.5 K (PT Towers)	Estimated costs for four generation stations with three load stations $50 K Commercial Cable Cost $5 M Space qualified cable
Launch Costs	$850 M	$520 M	$100 K / kg – To Moons Surface
Total Cost	$860 M	$540 M	

One of the leading new technologies is wireless power transfer (WPT) or power beaming**.** Directed WPT was first proposed by Nickola Tesla (U.S. patent No. 685,954, Nov. 1901)[1]. In

1961, Bill Brown published an article on WPT using microwaves, and in 1964 demonstrated the capability by powering a tethered subscale helicopter for 10 hours [2].

> *"Key to this flight was the "rectenna" which was invented to absorb the microwave beam and simultaneously convert it to DC power." [2]*

While several documented studies have explored WPT applicability for space-to-ground or space-to-space power transmission systems, there have been very few papers published on lunar and terrestrial applications. One commercial company (PowerCast LLC) is in the process of developing a rectenna concept to power low wattage consumer goods, such as hand held devices. This type of system has limited range and can only transfer milliwatts of energy. The Defense Advanced Research Projects Agency (DARPA) has also funded an effort to harvest power using a rectenna placed in the side lobes of a transmitting antenna. Several additional WPT background references not directly cited in the text are included at the end of this report.

It is important to note that several near-field wireless powering schemes exist, but are not applicable to this mission and are therefore not discussed. These include inductive powering and the more recent "resonant" power transfer being researched by an MIT group, which is a weakly coupled transformer requiring short range.

For the purposes of this study, we consider far-field high-frequency radio-wave powering systems which incorporate highly-directional antennas for beaming, high-efficiency transmitters, and high-efficiency receiving rectifiers.

I.1. WIRELESS POWER TRANSMISSION SYSTEM DESIGN STUDY

Wireless Power System Requirements

The four key parameters identified for the wireless power transfer system design of interest are:

- Power must be beamed from four solar power generation stations to five fixed load stations;
- Power received at each facility must be at least 10 kW;
- Load stations must receive power from minimum of two generation stations;
- Distance between transmitters and receiver ranges from 0.5 km to 2 km.

The beaming frequency, transmit and receive apertures sizes, and overall architecture are parameters varied in this study to show trends and the potential optimization.

This study considers the following system aspects of a wireless beaming system with respect to the specifications given above:

1. Top level system architecture – this includes a discussion of the distribution of power from 4 solar power generation stations to 5 load stations, as well as a high-level system block diagram.
2. Solar power generation – overviews the state of the art in PV arrays and discusses requirements in terms of size and mass for the required 50kW of received power at the five sites.

3. Power management and distribution – describes how the output of the PV arrays is managed and distributed to microwave transmitters.
4. System grounding on the lunar surface – electrostatic and other means are discussed.
5. Energy storage – describes alternatives and strategies for storage at the transmitter and site ends.
6. RF wireless power transmission – consists of a discussion of choice of frequency, transmitter technology, transmit aperture for given distance, towers for line-of-sight transmission, rectenna array size and DC reconfiguration. This is the central part of the study, but it cannot be considered properly without the other parts of the system.
7. System considerations including potential harm to astronauts and thermal issues are outlined for future more detailed study.
8. Mass and cost of the system is estimated. This is a very rough estimate since there is significant new work, and detailed analyses and design have not been performed.

I.2. Overall Architecture

The overall architecture for the lunar Wireless Power Transfer (WPT) system is shown in **Figure 1.1**. Four transmission towers power a total of five load stations, such that each facility may be powered by at least two towers, and each tower can power up to three facilities. Each tower can send power in up to three directions using three separate microwave transmitting antennas. Each arrow represents a directional microwave beam.

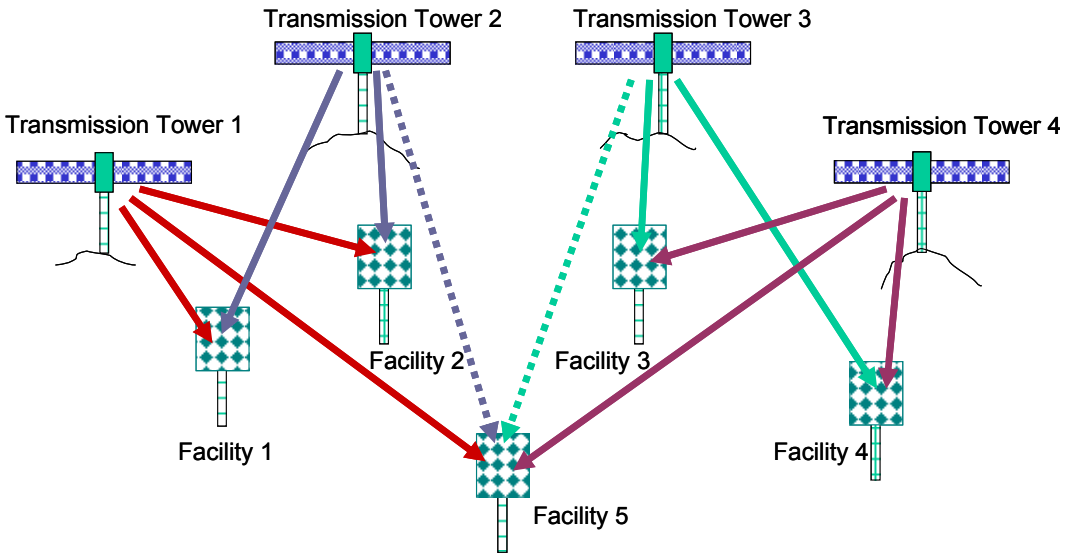

Figure 1.1. Top-level diagram of the notional lunar Wireless Power Transfer (WPT) system provides 10 kW to multiple load stations at distances between 0.5 and 2.0 km. Each arrow represents a directional microwave beam. The length of the arrow is an indicator of the aperture size of that particular transmit antenna – the larger the beaming distance, the larger the aperture for a given beaming efficiency.

The distances between the transmitters and rectenna arrays are between 0.5 and 2km, meaning that the farthest facility will be four times further with sixteen times more power attenuation than the closest facility (assuming identical aperture sizes). The farthest facility, #5, is powered by

four beams in this scenario, which enables all transmitters to have the same total output power, per Table 1. Alternatively, Transmitters 1 and 4 could produce more power than Transmitters 2 and 3, eliminating the beams shown in dashed lines in Figure 1.1. The numbers corresponding to this scenario are shown in parentheses in **Table 1**. The last row in the table includes beaming efficiencies, which are discussed in more detail in Section II. A modular transmitter approach would be advantageous since it allows tailoring of the transmitter size to the expected load distance.

Table 1. Transmitter power levels contained in different beams for two scenarios shown in Figure 1.1. In one case, all transmitters produce equal total power levels, each with three beams. In the second case, Transmitters 1 and 4 have three beams and produce more power than Transmitters 2 and 3, each with 2 beams (shown in parenthesis). For optimal efficiency, all apertures would be of different sizes.

	Transmitter 1	**Transmitter 2**	**Transmitter 3**	**Transmitter 4**	**Total power**
Facility 1	5kW	5kW			10kW
Facility 2	5kW	5kW			10kW
Facility 3			5kW	5kW	10kW
Facility 4			5kW	5kW	10kW
Facility 5	2.5kW (5kW)	2.5kW (0)	2.5kW (0)	2.5kW (5kW)	10kW
Total power	η_1 12.5kW (η'_1 15kW)	η_2 12.5kW (η'_2 10kW)	η_3 12.5kW (η'_3 10kW)	η_4 12.5kW (η'_4 15kW)	η 50kW

The most relevant parameter for comparing WPT with a traditional cable power transmission system is the overall efficiency and mass, with cost following. **Figure 1.2** shows an overall system block diagram, with the relevant efficiency budget given for the box with dashed lines, which shows the portion of the system most appropriate to compare to a traditional power transfer system.

The total WPT efficiency for a single channel can be defined as

$$\eta = \eta_T \cdot PCE \cdot \eta_{Beam} \cdot \eta_{Rect} \cdot \eta_{PM} = \frac{P_{DC,in}}{P_{DC,out}}$$

Table 2 describes the efficiencies that can be separated out and characterized separately.

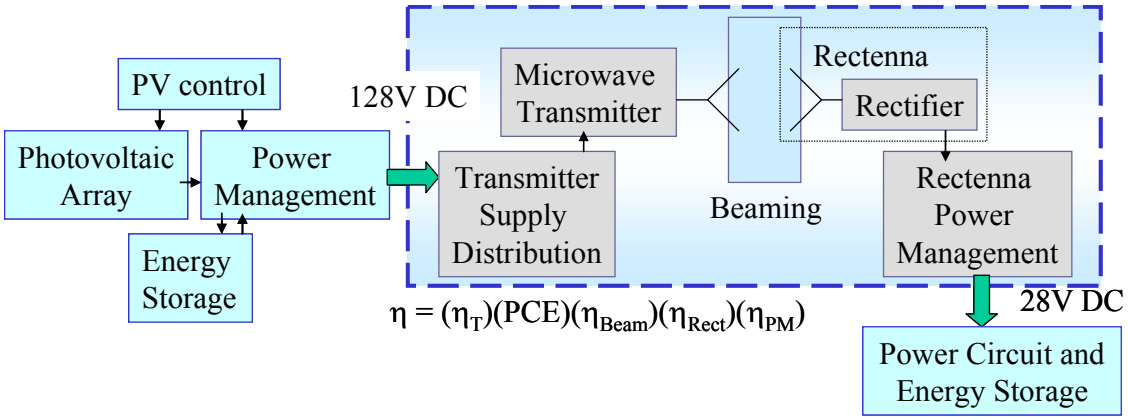

Figure 1.2. Overall power transfer system block diagram for a single powering beam (powering channel). The dashed shaded block outlines the portion of the wireless power beaming system that should be compared to traditional power transmission lines.

Table 2. Efficiency budget.

Efficiency	Description	Max Demonstrated
$\eta_T = \frac{P_{RF,antenna}}{P_{DC,in}}$	Total microwave transmitter DC-RF conversion efficiency, where $P_{RF,Out}$ is the RF power delivered to the transmitting antenna.	70-80% power and frequency dependent [3,4]
PCE	Power-combining efficiency of the transmitter (no single RF source provides the required multiple kW)	80-90%, combiner-type dependent [5]
$\eta_{Beam} = \frac{P_{RF,Trans}}{P_{RF,Rec}}$	Beaming efficiency between the transmit and receive apertures, including the free-space propagation loss	About 80% for far-field (see next section)
$\eta_{Rect} = \frac{P_{DC,Rectified}}{P_{RF,Rec}}$	Rectification efficiency of the rectenna, where the input is the received RF power at the aperture, and the output the non-regulated DC power	80% [6]
$\eta_{PM} = \frac{P_{DC,out}}{P_{DC,Rectified}}$	Rectenna power management efficiency required to produce given fixed output voltage	85-90% dependent on rectenna number and power [7]

The third column shows best reported results for efficiencies, which are not at consistent frequencies, power levels, etc. Thus, these numbers show an upper limit on the overall efficiency of WPT of around 45%. A relevant comparison needs to take into account grounding, mass, cost/ease of deployment and reconfigurability, in addition to the efficiency (loss). The WPT approach has the potential to have advantages in terms of grounding, reconfigurability, mass and cost.

I.3. SINGLE BEAMING CHANNEL ARCHITECTURE

The envisioned lunar WPT system consists of several wireless powering channels, each one depicted in some detail schematically in **Figure 1.3**. A channel consists of an advanced solar arrays, power system based on the International Space Station (ISS) architecture (energy storage, Sequential Shunt Unit (SSU) & Battery Charge/Discharge Units (BCDU), Main Bus Switching Unit (MBSU), Remote Power Distribution Assemblies (RPDAs), Secondary Power Distribution Assemblies (SPDAs)), solar array control, power management and distribution (PMAD), high efficiency RF transmitters, high-directivity transmit antennas, and large-area rectenna arrays with associated DC combining and regulation. The system architecture also addresses the need for a transmission tower structure, grounding, energy storage, static dissipation, and thermal management.

The blocks shaded in blue in **Figure 1.3** are directly related to the wireless power beaming system. Some of the components in the dashed boxes containing the RF transmitters and rectennas would need to be specifically designed for WPT. Some subsystems would likely be the same no matter what power distribution method were to be chosen, including cables.

I.4. SOLAR POWER GENERATION, POWER MANAGEMENT, AND GROUNDING ON THE LUNAR SURFACE

As shown in Figure 1.3, the solar power generation and power management and storage will not differ significantly between a WPT system and other power transmission systems. Nevertheless, it is important to briefly overview some possibilities and challenges in these areas, as well as the issue of grounding.

The solar power photovoltaic (PV) generation facility is one of the most mature technologies employed in the WPT system. A typical photovoltaic system has planar solar arrays for power generation and chemical batteries to store excess solar array energy during periods of sunlight and provide power during periods when the load station is in shadow. It is expected that the batteries will only provide survival power during eclipse.

For a future lunar power system, one should consider using a new technology known as a Stretched Lens Arrays (SLA). This solar array technology uses a Fresnel lens and high efficiency multi-junction cells to provide superior PV performance. The Fresnel lens (concentrates the Sun, 8 to 1), is light weight, scalable with a capacity of 100's of kW's, provides outstanding radiation resistance, has a built in passive thermal management (radiator), has a high specific power (~300 W/kg) and can operate at high voltages (300 – 600 V). A single SLA is shown in **Figure 1.4**.

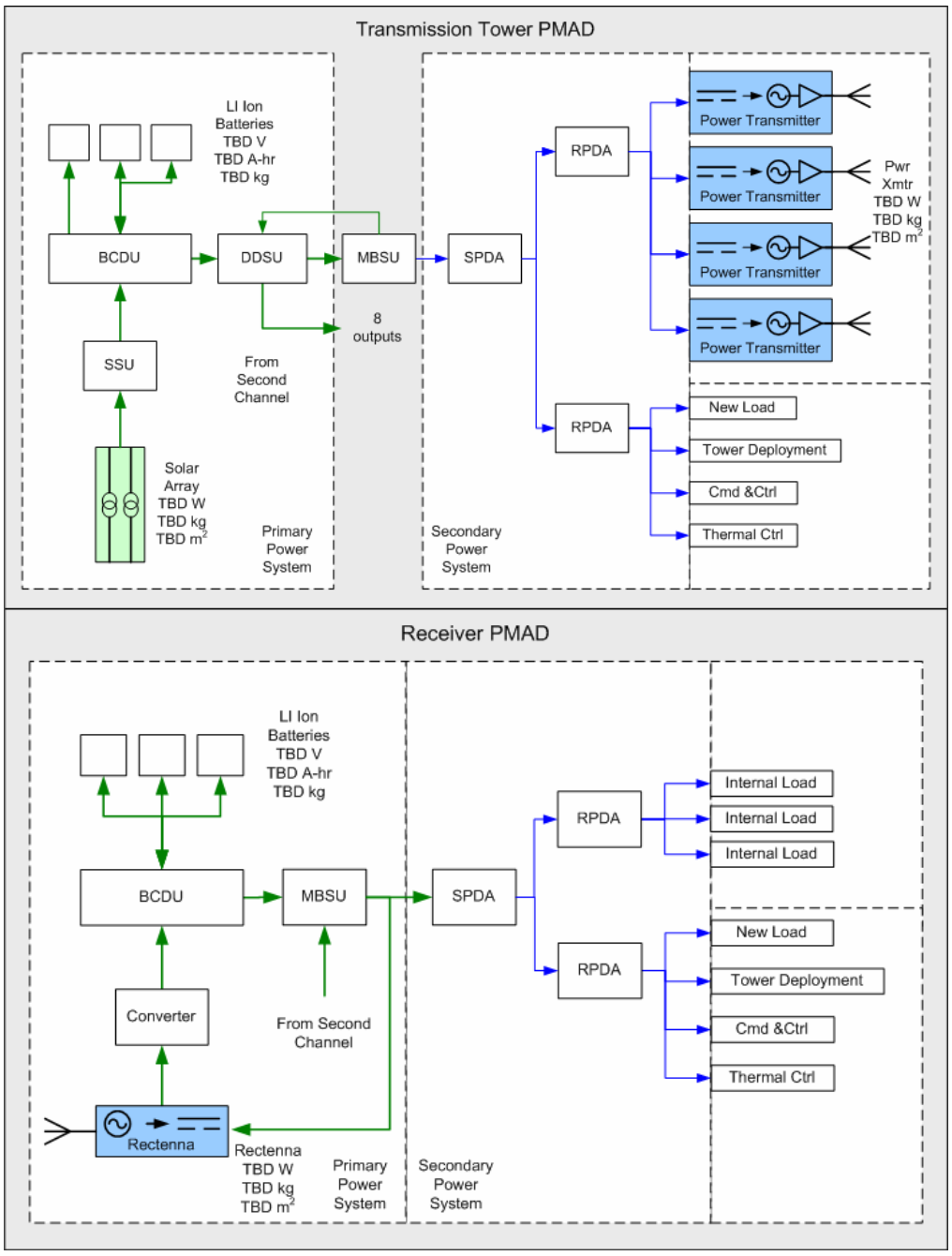

Figure 1.3. Block diagram of WPT channel. Several such channels power a single remote facility. The top figure shows the transmitter system block diagram, starting from solar array to a transmitter antenna or array. The bottom figure shows the receiver, starting from a rectenna array with reconfigurable DC summing, to the remote site loads.

Figure 1.4. Single cell stretched lens array enables low mass high efficiency power [8].

For a lunar power generation station, Entech, ATK and NASA (Glenn Research Center) have developed a modular 2.5 m X 5 m 4 kW SLA square rigger (SLASR) array as shown in **Figure 1.5**. This modular SLASR is highly compactable and is expected to be easily mass produced. Future SLA concepts are expected to have specific power levels in excess of 1000 W/kg.

Figure 1.5. Single Cell Stretched Lens Array enables low mass high efficiency power generation [9].

The power management and distribution (PMAD) system for WPT is very similar to the ISS PMAD System. Since the ISS PMAD system is modular, much of the hardware can be used "as is" with little or no modification for the lunar WPT system. A single PMAD channel or "set" of ISS PMAD hardware can supply the required fault protection, redundancy, and power for one lunar load station exceeding 10kW. A multiple set of modular ISS PMAD channels can supply the required fault protection, redundancy and power for one lunar solar power generation station exceeding 80KW. The main modifications that would be required to a baseline ISS PMAD channel are as follows:

- New concentrator solar arrays will be used instead of conventional planar solar arrays
- New technology Lithium Ion batteries will be used instead of conventional Nickel Hydrogen batteries
- Software modification to support new technology Li Ion batteries and new concentrator Solar Arrays will be required in the form of current and voltage regulation set points and battery charging algorithms.
- The Solar Array "Sequential Shunt Unit" (SSU) would require modification for load current and number of channels in order to adapt to the new concentrator solar arrays

- The "Battery Charge/Discharge Unit" (BCDU) would require modification to support the new Li Ion Batteries.
- The DC Switching Unit (DCSU) would require modification for fault protection software and potentially hardware modifications as well.
- Quantities of Main Bus Switching Units, DC-DC Converters and Remote Power Controller Modules will be fewer than the ISS requires.
- Modification of hardware to replace obsolete components will also be required in some cases.

Grounding - The lunar environment presents difficult problems in the grounding of electrical systems. Since the lunar regolith is in general a good insulator, terrestrial concepts such as single point grounds connected to simple buried rods are not viable on the moon. Additionally, the surface of the moon is highly charged due to interaction with the local plasma environment and solar radiation-induced photoemission of electrons. Such surface static charging is periodic over both short and long timescales. During the lunar day, the surface typically charges positively, while at night the surface charges negatively. Due to orbital variations, the moon has periods of time where interaction with the geomagnetic plasma sheet of the earth creates an enhanced charging environment. During these cycles, which peak approximately every 18 years, the lunar surface becomes even more charged. It is believed that the static potential of the lunar surface may vary daily between +10 and -600 volts [10] and possibly to several kilovolts [11].

Lunar surface charging is not fully understood and has only been observed indirectly. During the Apollo and Surveyor missions a glowing haze was observed above the limb of the moon which is believed to have been caused by charged dust particles lofted high above the surface [10]. Note however that the Apollo and Surveyor missions occurred during a low point in the 18-year cycle, so these effects are likely to be more pronounced during a cycle peak. The next cycle peak is expected between 2012 and 2019 [11].

Grounding can be defined as the electrical connection of the primary reference of the electrical device to a large enough conductive mass such that charges transferred to the mass do not result in a significant increase in the overall charge of the mass. Thus the reference maintains a charge that is stable during the operation of the device. Such a stable reference is useful for reducing electrical noise, and preventing a build-up of charge that could cause arcing to other areas or present a danger to operators or other systems.

Note that power beaming has significant grounding advantages when compared to transmission via cables. Since there is no physical connection between the transmitting station and the receiving station, different ground potentials for each will not be an issue. For cables, variations in static charging environments between the two sites (due for example to being in shade and sun) could cause large return currents to flow. This can drive the need for additional circuitry to handle such currents and also result in stations becoming highly charged with respect to their local environment if the capability of the ground is limited.

Various approaches to lunar grounding have been proposed, some of which could properly be characterized as charge management rather than traditional grounding. Each of the approaches described below will require further study to determine which are truly viable:

- Use of grounding rods with the injection of conductive materials into the lunar regolith.

- Use of ion/electron guns to expel positively or negatively charged ions.
- Ion Proportional Surface Emission Cathode (MIT) [12, 13].
- Field Effect Emitters (Space Systems/Loral) [14].

I.5. WPT CHANNEL PARAMETERS

The main sub-system for a single wireless powering channel are discussed here, with references to state-of-the art results. Section II presents more detailed discussion of the WPT channel.

Microwave Transmitter – The transmitter takes DC input and converts it to a radiated RF output. It consists of a DC-RF conversion oscillator, which is typically low-power and followed by a gain stage and finally a power amplifier (PA). The following considerations are relevant in this case:

- Since the DC input is 128V, some DC-DC conversion is needed to supply the required voltage needed for microwave devices (typically 8 to 48V range). This DC-DC conversion circuitry can be very efficient (98% is relatively easy to demonstrate).
- The main contributor to the loss is the Power Added Efficiency (PAE) of the output stage PA. A number of new wide bandgap semiconductor technologies are showing excellent efficiencies and power levels in the lower microwave range (commercially available) as well as in R&D labs (e.g. Northrop Grumman Space Technologies) [15].
- Both the device and circuit are important for the efficiency budget, and since no linearity or noise requirements exist in this case, a ultra-high efficiency saturated switched-mode PA will give the best efficiency [16].
- Power combining will be necessary, and there are several options at the circuit level or upon radiation.

Transmitter Antenna – The size of the antenna is determined by several factors: beaming efficiency for a given range, transmitted power per unit area, ease of fabrication and deployment, etc. For optimal efficiency with a large aperture, spatial power combining is a good choice, e.g. [5, 17]. Power combining efficiencies of great than 80% have been demonstrated in spatial combiners [18, 19]. An array of narrowband planar printed antennas, e.g. patches, is a good candidate for this approach. In the next section some possible power levels and array sizes are given at several frequencies. Ultimately, they will be driven by transistor technology and $/watt of power.

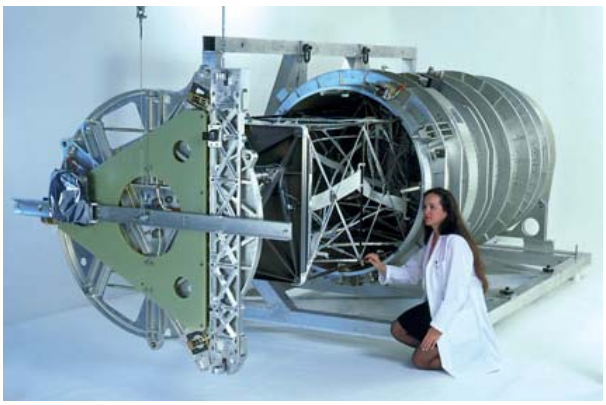

Figure 1.6. ATK's FAST Mast enables rapid deployment of the RF transmission tower [21].

Beaming – the beaming efficiency can be high for line-of-sight links. On the lunar surface, line of sight for a 2-km range requires towers for the transmitters. We also envision towers for the rectenna receivers in order to provide safety of personnel at the load stations. As an example, ATK's Folding Articulated Square Truss (FAST) Mast technology, installed on the International Space Station in2006, allows for compact stowage length less than eight feet when

fully retracted and more than 115 feet when fully deployed [20]. The FAST shown in **Figure 1.6** is attractive not only for its ISS heritage, but also because it utilizes the following [22]:

- A motor driven, internally-threaded canister shell to extrude the boom
- Stowed and transitioning portions of boom are fully contained within canister
- Near full stiffness and strength throughout deployment
- Large deployment push force capability
- Remotely retractable and deployable
- No rotation during deployment
- Typical applications include solar array deployment

Rectification – The transmitted power density is focused on an array of rectennas in the far field of the transmitter. An integrated antenna and rectifier is usually referred to as a *rectenna,* as shown in **Figure 1.7a**. Rectification of microwave signals for supplying dc power by high power beaming has been researched for several decades, and a good review of earlier work is given in [23]. In power beaming, the antennas have well-defined polarization, and high rectification efficiency is enabled by single-frequency high microwave power densities incident on an array of antennas and rectifying circuits. Applications for this type of power transfer have been proposed for helicopter powering, solar-powered satellite-to-ground power transmission, inter-satellite power transmission including utility power satellites, mechanical actuators for space-based telescopes, small dc motor driving and short range wireless power transfer (see references at the end of the reference list). Linear, dual-linear and circular polarization of the receiving antennas were used for demonstrations of efficiencies ranging from around 85-90% at lower microwave frequencies to around 60% at X-band and around 40% at Ka-band.

For most rectennas and arrays reported to date, the antenna is matched to the diode around one frequency at a well-defined polarization and assuming relatively high incident power levels. For example, the rectenna shown in **Figure 1.7b** is linearly-polarized and designed to operate at 5.8GHz with an incident power of 50mW corresponding to an incident power density of around 3.2mW/cm^2, assuming a dipole effective area of $\lambda^2/8$. In this case, the incident wave carries enough power to turn on the diode and rectification efficiency can be very high (>80%).

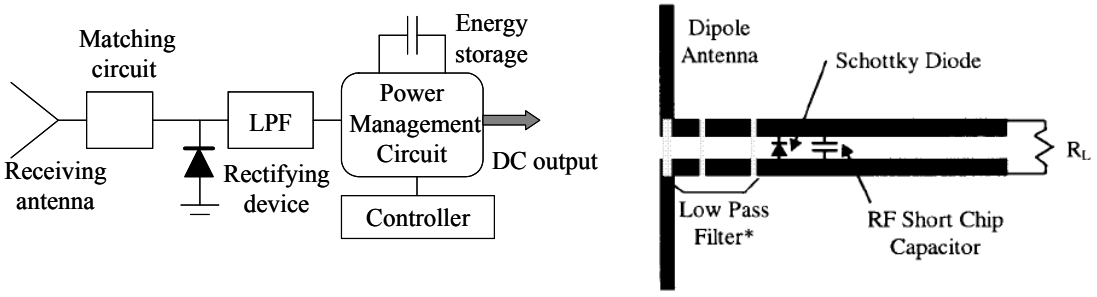

(a) (b)

Figure 1.7. (a) Schematic of a rectenna and associated power management circuit. The incident wave is received by the antenna, coupled to the rectifying device, and the low-pass filter (LPF) ensures that no RF is input to the power management circuit. A controller provides input to the power management circuit, which enables storage of the received energy over time, and delivery of DC power at the level and time when it is needed. (b) An example of a dipole rectenna for 5.8GHz narrowband operation [24].

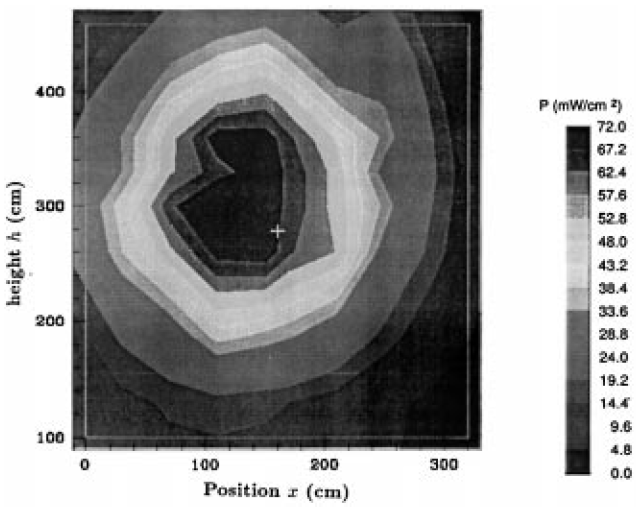

Figure 1.8. Measured power flux from parabolic transmitter at receiving rectenna. The power exhibits radial symmetry, with peak power flux occurring in the center (details can be found in reference [25]).

For the proposed beaming study, the following needs to be considered:

- The rectenna arrays will be very large, planar and deployable.
- The beam from each transmitter will non-uniformly illuminate the rectenna array aperture. An example of a measured beam specifically used in wireless power transfer is shown in **Figure 1.8** [25]. The exact beam pattern would off course depend on transmitter antenna design.
- This implies that not all rectennas will be receiving the same power, and thus might not be operating at optimal efficiency. A solution is to design the rectenna to be modular, i.e. that a subarray of rectennas is connected to a local powering circuit which presents an optimal load at the particular power level that the rectenna elements are receiving on average. Details are given in Section II and Appendix B.
- The powering beam needs to be maximally absorbed by the rectenna aperture, implying direct integration of antenna elements with rectifying elements. The rectenna in Figure 1.7(b), for example, does not meet this requirement as the filtering and matching circuit takes up too much real-estate at the expense of absorbing area. The design of the integrated rectenna element requires a specific procedure which is not well established in the field, although a good methodology for low power is described in [27]. The procedure involves a load-pull measurement that provides an empirical nonlinear device model. The diode impedance can then be determined for a given power, and the antenna impedance designed to directly match this optimal diode impedance.
- When several transmitters are beaming power to a rectenna aperture, the combined incident field will change as compared to that of a single transmitter case. The differences among elements will be even larger, and thus the modular approach is essential if efficiency is to be optimized.

I.6. SYSTEM CONSIDERATIONS

Some additional system considerations are summarized in the **Table 3** below.

Table 3. System level considerations for the lunar WPT system.

System Level Considerations	
Astronaut Considerations	• Safety issues for astronauts walking through the beams • Uncontrolled pointing of the RF transmitter • Human capabilities analysis and plan • Antenna side lobe and reflected power safety issues
Transmission Tower	• Deployment in 0.6g • Testing in 1g
System Design	• Packaging for launch /storage • Transportation to final location on lunar surface • Deployment at landing site – Automatic vs. manual • Assembly Process (Cable management) • Antenna alignment / point away approach • Grounding of the various system elements • Voltage regulation approach
RF WPT Operations	• RF Transmitter / Rectenna Pointing • Assembly Process • Maintenance
System Efficiency	• Best common voltage for the system • Load shedding and management approach
Thermal Control System	• Array and transmitter thermal management • Electronics thermal management
Other	• Dust mitigation in the presence of large static fields • Power harvesting of the side lobes • Energy storage sizing and selected battery technology • RF and sub-RF EMI mitigation • Control of the system via WiFi or other means

II. WPT CHANNELS

In this section, some estimates are given for the transmitter and transmitting antenna efficiencies, beaming efficiency and receiving rectenna efficiency, assuming a single powering channel. Beaming efficiency is discussed first, since this consideration determines the relationship between the transmitting and receiving aperture sizes for a given frequency (wavelength), then range (beaming distance).

II.1. BEAMING EFFICIENCY AND APERTURE SIZE

Assuming a beaming frequency f at which the free-space wavelength is λ, the required beam diameter d for a power beaming range R can be determined using the antenna theorem $A/D = \lambda^2/4\pi$, where A is the effective area of the antenna and D the directivity. Assuming a 100% aperture efficiency, the half-power beam-width of a symmetrical-beam antenna can be calculated approximately to be, in degrees from $D \approx 32{,}000/\theta^2$. For different power beaming ranges, the aperture size can now be estimated using

$$\tan\theta_{-3dB} = d/R \Rightarrow 2d = aperture.$$

The following simple estimate can be used for beaming efficiency and determining the required aperture size. If the transmit and receive antennas are in each other's far field, one can define (from the Friis formula) a beaming efficiency as

$$\eta_{Beam} = \frac{P_{RF,Trans}}{P_{RF,\mathrm{Re}c}} = \frac{A_{Trans} A_{\mathrm{Re}c}}{\lambda^2 R^2},$$

where the effective areas of the antennas are assumed to be equal to their geometric areas for this estimate. The distance *R* needs to be in the far field for this to be valid. For a distance (range) of 2km, assuming 2GHz, 5GHz and 10GHz beaming frequencies, and a 80% beaming efficiency, **Table 4** shows possible resulting aperture sizes. (For more details on the derivation, see Appendix A.)

These specific frequencies were chosen as examples in order to illustrate scaling: from a beaming standpoint, the higher frequencies (smaller wavelengths) are clearly better. However, the transmitters and rectennas are less efficient at the higher frequencies. In fact, at X-band the best rectenna efficiencies were about 60% and it would be difficult to get more than 60% efficiency from a power amplifier with a few watts at this frequency.

The following is noted for the calculations in Table 4:

- For each frequency, the beaming efficiency is set to 80%, i.e. $A_T A_R = 0.8\lambda^2 \cdot (2km)^2$
- The first row for each of the three frequencies is the case of equal transmitting and rectenna (receiving) apertures;
- The estimate the number of antenna elements, assuming both apertures are arrays, an element spacing of one half of a free space wavelength is assumed both at transmitter and rectenna apertures;
- The directivity is calculated from $A/D = \lambda^2/4\pi$ assuming that the effective area of the transmitting antenna is equal to its geometric area;
- The far field condition $FF \sim 4A/\lambda$ is calculated w.r.t. the transmitting aperture, since the rectenna elements have individual detectors, and RF-wise they are not in an array (only the DC adds);
- The far field condition is not met for all cases when apertures are of equal size. This implies that the estimates used here are not valid (Fresnel zone equations should be used);
- The half-power beamwidths are calculated from $D \approx 32{,}000/\theta^2$, which is an assumption. A more precise beamwidth can be calculated once the transmitting antenna architecture is determined;
- Based on the 2-km range and the half-power beamwidth, the spot size of the transmitting beam on the rectenna surface is calculated. A system design would have an increased rectenna size, in order to capture as much power as possible of the beam, thus increasing the beaming efficiency. Note also that the beam power density across the rectenna aperture will vary according to a sinc^2 function.

Table 4. For an 80% beaming efficiency, and three beaming frequencies, several transmit and receive apertures can be considered. The borderline far field at the 5GHz frequency is the baseline configuration used for mass and cost estimates provided in Section III.

Frequency/ Wavelength	AT AR	Transmit aperture No. of el. N Directivity D	HPBW and Far Field	Receive aperture No. elements N	Spot size
2GHz / 15cm	72,000 m^4 Not in far field at all	16m x 16m N=106 x 106 D=51dB	0.48° FF~14km!	16m x 16m N=106 x 106	d=17m
	Borderline far field	10m x 10m N=133 x 133 D=47dB	0.77° FF~2.7km	27m x 27m N=360 x 360	d=27m
		5m x 5m N= 67 x 67 D=41dB	1.59° FF~670m	54m x 54m N=720 x 720	d=55m
5GHz / 6 cm	11,520m^4 Not in far field	10m x 10m N=333 x 333 D=55dB	0.32° FF~3.5km	10m x 10m N=333 x 333	d=11m
	Borderline far field	5m x 5m N= 150 x 150 D=49dB	0.63° FF~1.7km	21m x 21m N=700 x 700	d=22m
		3m x 3m N=100 x 100 D=44.8dB	1° FF~600m	36m x 36m N=1200 x 1200	d=36m
10GHz / 3cm	2,880 m^4 Not in far field at all	7.3m x 7.3m N=485 x 485 D=58dB	0.23° FF~7.1km	7.3m x 7.3m N=485 x 485	d=8m
		3m x 3m N=200 x 200 D=50dB	0.51° FF~1.2km	18m x 18m N=1200 x 1200	d=18m

II.2. TRANSMITTER AND TRANSMITTING ANTENNA

The main considerations in the transmitter are power amplifier device technology, efficiency and cost; power amplifier circuit architecture and efficiency; and power combining efficiencies, as discussed below.

Devices

Power devices for high-power microwave sources can be either tubes, solid-state or solid-state driven traveling wave tubes (TWTs). The mass, reliability, efficiency and continuous

improvements in solid-state device technologies, along with considerations in Table 2, points to the use of transistor amplifiers in active antenna arrays.

Standard transistors with tens to hundreds of watts of output power at lower microwave frequencies are LDMOS (cell-phone base stations) or GaAs FETs (tens of watts at X-band in class AB). The LDMOS devices cannot operate efficiently above about 2GHz, while GaAs FETs are expensive and limited in power. On the other hand, wide-bandgap semiconductors such as GaN and SiC have better intrinsic material properties than standard Si LDMOS transistors, i.e. larger energy gap (support higher internal electric fields before breakdown), lower relative permittivity (lower capacitive loading), higher thermal conductivity (higher heat handling), and higher critical electric fields (higher RF power) [27]. High voltage operation and high power density with low parasitic reactance translate into robust devices that can withstand high-stress conditions typically associated with switched-mode operation. For example, in ultra-efficient Class–E mode, the peak voltage across the device can be more than 3.56 times higher than the supply voltage. The supply voltage must then be limited by this factor (VDSS/3.56 were VDSS is the absolute maximum drain-to-source voltage). Therefore, devices with high breakdown voltage are ideal for efficient modes of operation.

A brief overview of some available devices is given in **Table 5**, although it should be noted that the cost quoted here is for small quantities.

Table 5. Comparison of transistor power levels, frequencies, voltages, and costs.

Transistor Type	Manufacturer(s)	Power Levels	Frequency	Voltage	Cost
LDMOS	Freescale, Agera, Ericson and many others	30, 60, 100W, 200W	<2GHz in high eff. mode	28V	$1.8/W
GaN on Si HEMT	Nitronex	25W, 50W, 100W	To about 4GHz	28V and 48V	$5/W
GaN on SiC HEMT	Eudyna, RFMD, TriQuint, Cree	10W, 30W, 60W, 100W	To about 3.5GHz	28-48V	$7/W
SiC MESFET	Cree	60W	Claim to 8GHz	28V-48V	$9.5/W
GaAs MESFET	TriQuint, NEC	6-10W	Up to X-band	10V	$15.2/W

A number of other defense contractor companies produce GaN devices at higher frequencies (there is a successful DARPA Wide-bandgap program). For example, BAE Systems has broadband GaN devices with around 10W up to 20GHz, while Northrop Grumman Space Technologies (formerly TRW) have produced GaN on SiC devices with close to 20W as high as 30GHz. TriQuint also produces GaN on Si targeting X-band. These are still in the development stage, but improvements have been happening very fast. GaN may not be space qualified yet, but Northrop Grumman will certainly have that focus. GaAs is still an option, with higher cost per watt of power. The remainder of the transmitters consist of VCOs (low-cost components from, e.g MiniCircuits), and some gain and driver stages. These only contribute to the efficiency minimally, since they are low power, and their cost is low compared to the power amplifier.

Power Amplifiers

The highest efficiency power amplifiers demonstrated to date operate in switched mode (classes E, D etc.). These are highly saturated nonlinear amplifiers with high additive phase noise. For powering applications, linearity and noise are not relevant, and the high efficiency of class E and tolerances to small differences in circuit parasitic parameters give this mode an advantage, e.g. [19]. In class E operation, the transistor is either on or off, with a minimal amount of time during a period where the product of voltage and current through the device is non-zero. Unlike in class C, the maximum output power of the device only needs to be sacrificed by 0.5dB or so.

The disadvantage of class-E mode of operation for this particular application is that the high efficiency is achieved at the expense of operating at about 3 to 5 times below the specified device maximal frequency of operation. For example, a device that is normally operated in class AB mode at 2GHz will perform well in high-efficiency switched mode anywhere between 0.5 and 1 GHz. With current device trends, it is likely that 5GHz will be an appropriate frequency for high efficiency with tens of watts per device in a few years, and 10GHz is not out of the question.

Mass: Northrop Grumman Space Technologies has produced 3-D stacked power amplifiers which are only a few tens of grams in mass (Dr. Dwight Streit, Vice President, *personal communication*, February 2008). This is achieved with a new packaging technology, and similar approaches can be adapted to the power beaming transmitters.

Antennas and Active Arrays With Spatial Power Combining

Given the numbers in Table 4, a high-level transmitter and antenna design is now discussed.

- Consider the middle frequency of Table 2 (5GHz) with 150x150 elements (a 5-meter square aperture) at a half-wavelength spacing for the array elements.
- For a single powering beam that delivers 5kW of power to a facility, and accounting for 80% beaming efficiency and 80% rectification efficiency, the transmitted power needs to be about 7.8kW.
- If every array element contained a high-efficiency amplifier, this would imply only 350mW per element.
- This is however not a practical approach, since it would require feeding 150x150 elements.
- We thus consider an array of modules. Assuming one can implement a low-loss 1:16 divider (as in [19]), the transmit array antenna would consist of 1400 modules.
- Each module will then need to radiate 5.6W of power. This is a very reasonable task, but still implies a large number of feeds. A more extensive trade study, including the type of antenna element, how it would be deployed, etc., is required. **Table 6** provides a few estimates in terms of subarray size, number and power, for a total of 150 x 150 elements at 5GHz, assuming a beaming efficiency of 80% and a rectifier efficiency of 80%, with 5kW of power per beam. This assumes a 100% power combining efficiency for the modules in the array.

Table 6. Estimates of sub-array quantities and transmitted power.

Number Of Subarrays	Number Of Elements Per Subarray	Power Transmitted Per Subarray
350	64	22 W (28 W)
175	128	45 W (56 W)
130	170	60 W (75 W)

The power from each module from the table above is radiated and combined with the radiated power from the other modules via spatial power combining. It has been shown, e.g. [5], that power combining efficiency degrades with the number of stages for circuit combiners and remains roughly constant for spatial combiners, with combining efficiencies demonstrated in the 80% range. This implies that the power levels in the above table need to be increased to the numbers in parentheses.

II.3. RECTENNA DESIGN AND BASIC PROPERTIES RELEVANT TO BEAMING

In a load station's power receiving array, the number of elements can be very large, since there is no RF combining network that can introduce loss. Instead, the rectified DC is combined. The modular approach for this design would be as follows:

- Assume an aperture size for the rectenna. For example, take a 20m x 20m rectenna aperture (Table 2, 5GHz, middle case).
- Knowing that 5kW (times the rectification efficiency) of power is incident over the aperture, the resulting incident power density assuming uniform illumination (which is not the case, but gives an average value) is calculated. In this case, it will be on the order of $5mW/cm^2$.
- Calculate the power density per rectenna array element. In the given example, the $5mW/cm^2$ power density results in about 45mW per array element assuming half-wavelength spacing.
- This amount of power is sufficiently high to drive a rectifier diode operating point into a region of high rectification efficiency. This will off course depend on the antenna element in the rectenna, choice of rectifying device (most likely zero-bias Schottky diode), impedance match and DC load.
- Now assume an array with element spacing of half wavelength ($\lambda/2$ period), implying narrowband beaming.
- Find number of elements in a module of that size (in the example here, it is 700 x 700 elements).
- Next, assume illumination profile of main beam (varies between modules, assume constant per module). This can be obtained by simulation or measurement and is transmitter-dependent.
- For V=28V nominal output voltage, assuming 0.5-0.7V per element based on previous work, find how many elements are needed in a subarray of each module (maybe no sub-arrays are needed, but rather parallel connections to boost the power).

Rectenna Element

An example patch rectenna with two rectifiers (one for each linear polarization) in the unlicenced ISM band around 2.4GHz is shown in **Figure 2.1**. The rectenna is a 19mm x 19mm square patch, with a 6cm x 6cm square ground plane on a Rogers Duroid 6010 substrate (εr=10.2, thickness=50mil) chosen to reduce the antenna size. A Schottky diode is connected at each of the two centers of the two orthogonally-polarized patch radiating edges. A via isolated from the patch ground plane terminates each diode to RF/DC ground, and the DC output is taken from the RF short in the center of the patch. This rectenna operates with incident power levels as low as 10μW/cm^2 and is capable of powering a low-power wireless sensor, but very similar planar antennas with different diodes can be designed for higher power levels (e.g. [28]).

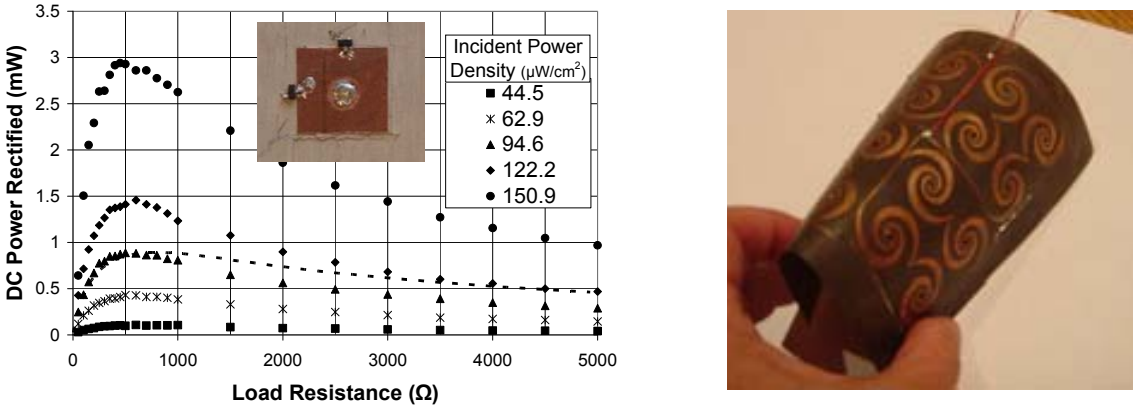

(a) (b)

Figure 2.1. (a) Measured rectified DC power as a function of the DC load for different incident power levels. A photograph of dual-polarized 2.4-GHz patch rectenna is shown in the inset. (b) A broadband rectenna array on a flexible substrate (no ground plane, bidirectional).

Remaining design issues are:

- type of substrate that is best for this application;
- type of metallization for the antenna;
- most appropriate way to attach diodes;
- is a ground plane needed on the back of the substrate, or would a reflector that is separated from the array by a half-wavelength vacuum layer be appropriate? This would imply that we do not need to work with patch antennas, but can use dipoles etc.
- how do we design the DC collection lines so that they do not couple to the RF. A patch antenna is a good choice, since the RF voltage null can be used for the DC.

Rectenna Modules

The rectenna arrays at the load stations will necessarily have large areas (per Table 4, e.g.). The diodes in individual rectenna elements can rectify only a limited amount of power and also produce a small voltage, so series/parallel combinations of many elements must inevitably be made. For V=28V nominal output voltage, assuming 0.5-0.7V per element based on previous work, about 56 elements need to be combined in series to produce the required voltage, which

implies over 8000 modules of this size for the entire rectenna array. With this requirement come several issues of electrical element interconnection within the array.

Distributed power management is designed and integrated at the subarray level to create integrated power modules that cover a range of power (e.g. 10-50W). The power management circuitry achieves two primary functions:

(1) peak power tracking of the rectenna subarray by matching the input impedance of the converter cell to the rectenna subarray low frequency output impedance and

(2) charge control for battery protection and long life charging.

The first function of impedance matching is required to achieve high overall system efficiency in the presence of wide variations in incident power density over the entire receiver aperture. A single power converter and management unit is used for both functions to achieve maximum system efficiency and to avoid the need to passively dissipate excess energy from the rectenna subarray in the case of battery overcharge. As a battery overcharge condition is approached, charge control is achieved by forcing a mismatch between the rectenna output and converter input impedance, causing the received input power to decrease to match the battery requirements. This removes the need for shunt dissipation elements and associated thermal dissipation considerations.

A trade-off study needs to be performed to determine the optimal series-parallel configuration and physical layout for each sub-array and the converter topology for maximum system efficiency. A brief outline of such a study is given in Appendix B.

II.4. OVERALL EFFICIENCY AND TRADES

The overall WPT system efficiency is given by

$$\eta = \eta_T \cdot PCE \cdot \eta_{Beam} \cdot \eta_{Rect} \cdot \eta_{PM} = \frac{P_{DC,in}}{P_{DC,out}},$$

where the individual efficiencies were discussed above. The expected efficiency budget is given in the **Table 7**.

The study so far has focused on a single wireless powering channel, i.e. beam. Referring to Figure 1.1, there will be multiple (at least 2) beams powering a single facility. The remaining study that needs to be performed is the effect of multiple transmitted beams incident on the same receiving rectenna aperture. There has been limited work on effect of simultaneous beams incident on rectenna arrays, with two beams at two different power levels and frequencies [26]. The results show that *in each* of 10,000 random trials, the efficiency *increased*, while the beam angles, frequencies and powers were varied. The increase was more pronounced for lower incident power levels. This implies that the overall rectification efficiency at the rectenna aperture in the presented case will increase with multiple beams, since the modules that are not capturing the peak power density of the beam with increase in efficiency.

It is interested to note that the rectenna array images the incident beam power profile. When elements are a half wavelength apart, the sampling of the incident beam is according to Nyquist

and the beam profile can be recovered fully. This direct mapping of the incident beam at the rectenna aperture has the potential to simplify dramatically the beam pointing of the transmitter.

Table 7. Expected efficiency budget for the lunar WPT system. Details used for the conclusions can be found in Tables 1-6 above.

Efficiency	Discussion of upper and lower bounds	Max expected	Trades
$\eta_T = \frac{P_{RF,antenna}}{P_{DC,in}}$	- upper bound is for lower microwave frequencies where the size increases - currently over 85% is achievable below 1GHz, but above 5GHz to get that same efficiency will require improvements in device technology	75–80%	- efficiency higher at lower frequencies, but arrays very large - cost lower at lower frequencies at expense of size
PCE	- depends on array architecture -for upper bound, which is achievable for narrowband case, all elements need to be designed for relatively broader bandwidth	80–90%	- high efficiency implies large number of elements, and the trade will be in the size of the module vs. number of modules
$\eta_{Beam} = \frac{P_{RF,Trans}}{P_{RF,Rec}}$	- for upper bound, it is borderline far field condition. This means that the incident field on rectenna aperture might differ from far-field approximation. - imaging beam pattern in situ can help achieve possibly higher beaming efficiencies where near field conditions might exist.	75–85% for far-field	- large range requires large apertures - large rectenna aperture that captures most of the beam power for high efficiency implies larger mass and cost
$\eta_{Rect} = \frac{P_{DC,Rectified}}{P_{RF,Rec}}$	- rectifiers need to all be in large-signal mode for upper bound. - for upper bound (optimal diodes and dense element packing), direct antenna-diode integration is needed.	75–80%	- dense element packing gives higher efficiency at expense of complexity and cost.
$\eta_{PM} = \frac{P_{DC,out}}{P_{DC,Rectified}}$	- upper bound has been shown for lower power levels, and it should be possible to get higher efficiencies for higher power levels - high efficiency will require high-quality component selection, which will increase the cost and might increase the mass.	85–95%	- reconfigurable parallel-series combining can optimize in-situ efficiency, at expense of complexity. - higher power at module level gives better module efficiency, but possibly lower overall array efficiency due to increased size of subarray
η (total)	- difficult to predict upper and lower bounds without further experimental and theoretical study	30–45%	- all of the above with additional parameters that require more study

III. MASS AND COST

The cost and mass of a traditional cable-based system and a wireless powering system are estimated using the 5-GHz beaming architecture for the case of a 5m x 5m transmitter aperture and a 20m x 20m receiving rectenna aperture (Table 2 in Section I). A 480-V transmission line cable system was used for comparison since it is optimal in terms of loss. More details of the analysis are shown in Appendix D, and a summary is shown below in Table 8.

The loss of the cable is increased due to temperature variations, as detailed in Appendix D. The mass of the cable is calculated for the case of bare cable. In reality, the cable comes with one line insulated with a thin PVC type insulation. The best solution might be to trench the cables, in order to suffer less voltage drop due to temperature changes, as well as enable operation at 220V. The associated loss is corresponds to an efficiency of ~60% (supporting details in Appendix C).

The lunar surface is composed of lunar regolith which has been shown to be a very good insulator, similar to exceptionally dry micron-fine silica sand. With a transmission line system, the source and the load are electrically connected and a return path to the source must be provided or current will not flow. The lunar surface is an insulator and will provide such a path. Conventional terrestrial transmission line systems ground at multiple locations, but do not use "Earth ground" for a current return path. Return lines are used exclusively for a current return path. In a WPT system, the source and the load are not electrically connected and rely on their respective "local" grounds.

Table 8. Summary of estimated mass and cost comparison between a conventional cable-based power transfer system and a wireless transfer power system.

System	Mass (kg)	Cost	Launch Cost	Efficiency
Traditional Transmission Line	7500	5.05 M	800 M	60%
WPT - Four Transmission Stations (Transmission Array) - Five Load Facilities (Rectenna Arrays)	4193	17 M	513 M	45%

IV. SUMMARY

A conventional transmission line architecture was developed so a comparison could be made between a lunar WPT system and a conventional transmission line system.
The identified advantages of a WPT system for this application are:
- reconfigurability (if the loads stations need to move, or stop operation, the antenna beam on the transmitter can be reconfigured to point in a different direction);
- overall mass is smaller by more than a factor of 2;
- there is no electrical connection between the transmitter and load in WPT, enabling local grounds.

V. REFERENCES

[1] J. Glenn, Ed., *The Complete Patents of Nikola Tesla,* Barnes and Noble Books, New York, 1994, pp. 346–360.

[2] http://www.mtt.org/awards/WCB's%20distinguished%20career.htm

[3] S. Pajic, N. Wang, P.M. Watson, T.K. Quatch, Z. Popovic, "X-band Two-Stage High-Efficiency Switched-Mode Power Amplifiers," *Microwave Theory and Techniques, IEEE Transactions on*, Vol. 53, No. 9, pp. 2899–2908, September 2005.

[4] N.D. Lopez, J. Hoversten, M. Poulton, Z. Popovic, "A 65-W High-Efficiency UHF GaN Power Amplifier," *accepted for presentation at the IEEE International Microwave Symposium,* Atlanta, June 2008 (4 pages).

[5] *Active and Quasi-Optical Arrays for Solid-State Power Combining*, eds. R.A. York and Z.B. Popovic, John Wiley and Sons, 1997. (Chapters 1 and 2)

[6] B. Strassner and K. Chang, "A circularly polarized rectifying antenna array for wireless microwave power transmission with over 78% efficiency," *IEEE MTT-S International Microwave Symposium Digest*, pp.1535–1538, 2002.

[7] T. Paing, J. Morroni, A. Dolgov, J. Shin, J. Brannan, R. Zane, Z. Popovic, "Wirelessly-Powered Wireless Sensor Platform," *European Microwave Conference Digest,* paper 1563, 4 pages, *presented in* Munich, Germany, October 2007.

[8] M.J. O'Neill, International Conference on Solar Concentrators for the Generation of Electricity or Hydrogen, Scottsdale, May 1–5, 2005, "ENTECH's Stretched Lens Array (SLA) for NASA's Moon/Mars Exploration Missions, Including Near-Term Terrestrial Spin-Offs."

[9] M.J. O'Neill, 4th World Conference on Photovoltaic Energy Conversion, Waikoloa, Hawaii, May 7–12, 2006, "Stretched Lens Array (SLA) for Collection and Conversion of Infrared Laser Light: 45% Efficiency Demonstrated for Near-Term 800 W/kg Space Power System."

[10] T.J. Stubbs (NASA Goddard), J.S. Halekas, W.M. Farrell, and R.R. Vondrak, "Lunar surface charging: a global perspective using lunar prospector data," Proceedings: *Dust in Planetary Systems*, Kauai, Hawaii, USA. September 26–30, 2005 (ESA SP-643, January 2007).

[11] M. Hapgood, "Modelling long-term trends in lunar exposure to the earth's plasma sheet," (Rutherford Appleton Laboratory, Chilton, U.K), submitted to Annales Geophysicae, July 31, 2007, Cornell University, arXiv:0705.0873v2 [physics.space-ph], available at http://arxiv.org/abs/0705.0873.

[12] USPTO Patent Application 20070090476, SURFACE-EMISSION CATHODES HAVING CANTILEVERED ELECTRODES, Michael W. Geis, et al. (Massachusetts Institute of Technology), 2007.

[13] D. Cooke and G. Ginet (Air Force Research Laboratory, Space Vehicles Directorate, Hanscom AFB, MA), "Ionospheric and magnetispheric plasma (and neutral density) effects," Proceedings: *NASA Solar and Space Physics and the Vision for Space Exploration Conference,* Wintergreen Resort, VA, October 16–20, 2005.

[14] M.J. Mandell, et al. (Science Applications International Corporation), F.K. Wong (Space Systems/Loral), R.C. Adamo (SRI International), D.L. Cooke et al. (Air Force Research

Laboratory, Hanscom AFB, MA), "Charge control of geosynchronous spacecraft using field effect emitters," Proceedings of the 45th AIAA Aerospace Sciences Meeting and Exhibit, January 8–11, 2007, Reno, Nevada.

[15] IEEE RWS Conference, Digest of Workshop on High-Efficiency Power Amplifiers, Orlando, Florida, January 20, 2007.

[16] F.H. Raab, P. Asbeck, S. Cripps, P.B. Kenington, Z. Popovic, N. Pothecary, J.F. Sevic, N.O. Sokal, "Power amplifiers and transmitters for RF and microwave," *IEEE Trans. Microwave Theory and Techn.,* Vol. 50, No. 3, pp. 814–826, March 2002.

[17] E. Bryerton, et al. "Efficiency of chip-level versus external power combining," *Special Issue on Low-Power/Low-Noise Circuits of the IEEE Trans. Microwave Theory Techn.*, pp. 1482–1485, July 1999.

[18] T. Mader, et al. "Switched-mode high-efficiency microwave power amplifiers in a free-space power combining array," E. Bryerton, M. Markovic, M. Forman, Z.B. Popovic, *IEEE Trans. on Microwave Theory and Techniques,* Vol. 48, No.10, pp. 1391–1398, October 1998.

[19] S. Pajic, Z. Popovic, "An efficient 16-element X-band spatial combiner of switched-mode power amplifiers," *IEEE Trans. Microwave Theory and Techn.,* Vol. 51, No. 73, July 2003.

[20] Retrieved from http://www.atk.com/Customer_Solutions_MissionSystems/cs_ms_space_dtb.asp, 2008-01-10.

[21] Image retrieved from http://www.atk.com/Customer_Solutions_MissionSystems/cs_ms_space_dtb.asp

[22] Retrieved from http://www.atk.com/Customer_Solutions_MissionSystems/documents/Coilable_Booms.pdf, 2008-01-11

[23] W.C. Brown, "The history of power transmission by radio waves," *IEEE Transactions on Microwave Theory and Techniques*, Vol. 32, No. 9, pp. 1230–1242, September 1984.

[24] J.O McSpadden, R.M. Dickinson, L. Fan, and K. Chang, "Design and experiments of a high-conversion-efficiency 5.8-GHz rectenna," *IEEE MTT IMS Digest*, Vol. 2, pp. 1161–1164, 1998.

[25] N. Shinohara and H. Matsumoto, "Experimental study of large rectenna array for microwave energy transmission," *IEEE Transactions on Microwave Theory and Techniques*, Vol. 46, No. 3, pp. 261–267, March 1998.

[26] J.A. Hagerty, F. Helmbrecht, W. McCalpin, R. Zane, Z. Popovic, "Recycling ambient microwave energy with broadband antenna arrays," *IEEE Trans. Microwave Theory and Techn.,* pp. 1014–1024, March 2004. ***Winner of the 2005 IEEE Microwave Prize for best paper of the year.***

[27] R. Trew, "SiC and GaN Transistors - Is There One Winner for Microwave Power Applications?" *Proceedings of the IEEE*, Vol. 90., No. 6., pp. 1032–1047, June 2002.

[28] C. Walsh, S. Rondineau, M. Jankovic, G. Zhao, Z. Popovic, "A Conformal 10-GHz Rectenna for Wireless Powering of Piezoelectric Sensor Electronics," *IEEE 2005 IMS Digest,* Long Beach, June 2005.

Additional References Related to Wireless Power Transfer

[1-1] N. Shinohara and H. Matsumoto, "Experimental study of large rectenna array for microwave energy transmission," *IEEE Transactions on Microwave Theory and Techniques*, vol. 46, no. 3, pp. 261–267, Mar. 1998.

[2-1] J.O. McSpadden, F.E. Little, M.B Duke, and A. Ignatiev, "An in-space wireless energy transmission experiment," *IECEC Energy Conversion Engineering Conference Proceedings.*, vol. 1, pp. 468–473, Aug. 1996.

[3-1] T. Yoo and K. Chang, "Theoretical and experimental development of 10 and 35 GHz rectennas," *IEEE Transactions on Microwave Theor and Techniques*, vol. 40, no. 6, pp. 1259–1266, June 1992.

[4-1] L.W. Epp, A.R. Khan, H.K. Smith, and R.P Smith, "A compact dualpolarized 8.51-GHz rectenna for high-voltage (50 V) actuator applications," *IEEE Transactions on Microwave Theory and Techniques*, vol. 48, no. 1, pp. 111–120, Jan. 2000.

[5-1] Y. Fujino, T. Ito, M. Fujita, N. Kaya, H. Matsumoto, K. Kawabata, H. Sawada, and T. Onodera, "A driving test of a small DC motor with a rectenna array," *IEICE Trans. Commun.*, vol. E77-B, no. 4, pp. 526–528, Apr. 1994.

[6-1] W.C. Brown, "An experimental low power density rectenna," *IEEE MTT-S International Microwave Symposium Digest*, pp. 197–200, 1991.

[7-1] J.O McSpadden, R.M. Dickinson, L. Fan, and Kai Chang, "Design and experiments of a high-conversion-efficiency 5.8-GHz rectenna," *IEEE MTT-S International Microwave Symposium Digest*, vol. 2, pp. 1161–1164, 1998.

[8-1] J.O. McSpadden and K. Chang, "A dual polarized circular patch rectifying antenna at 2.45 GHz for microwave power conversion and detection," *IEEE MTT-S International Microwave Symposium Digest*, pp. 1749–1752, 1994.

[9-1] B. Strassner and K. Chang, "A circularly polarized rectifying antenna array for wireless microwave power transmission with over 78% efficiency," *IEEE MTT-S International Microwave Symposium Digest*, pp.1535–1538, 2002.

[10-1] J.A Hagerty and Z. Popovic, "An experimental and theoretical characterization of a broadband arbitrarily-polarized rectenna array," *IEEE MTT-S International Microwave Symposium Digest*, vol. 3, pp. 1855–1858, 2001.

[11-1] J. C. Lin, "Radio frequency exposure and safety associated with base stations used for personal wireless communication," *IEEE Antennas and Prop. Magazine*, vol.44, pp.180–183, Feb. 2002.

[12-1] J.C.Lin, "Space solar-power stations, wireless power transmissions, and biological implications," *IEEE Microwave Magizine*, pp. 36–42, Mar. 2002.

[13-1] Retrieved from Global Security.org (http://www.globalsecurity.org/wmd/facility/doe_nts_schooner.htm) on 2008-01-28

[14-1] Retrieved from www.osti.gov (http://www.osti.gov/opennet/reports/plowshar.pdf) on 2008-01-28

[15-1] Retrieved from http://antwrp.gsfc.nasa.gov/apod/ap070623.html on 2008-01-28

APPENDIX A – BEAMING EFFICIENCY AND RECTENNA ARRAY CONSIDERATIONS

For a given aperture size Ai assuming a beaming frequency f at which the free-space wavelength is λ, the required beam size *d* for a power beaming range *Rij* can be determined using the antenna theorem $A_i / D_i = \lambda^2 / 4\pi$, where *Ai* is the effective area of the antenna of transmitter i and *Di* the directivity. Assuming a 100% aperture efficiency, the half-power beamwidth of a symmetrical-beam antenna can be calculated approximately to be, in degrees from Di=32,000/θ^2. For different power beaming ranges, the aperture size can now be estimated using $\tan\theta_{-3dB} = di / R_{ij} \Rightarrow 2di = aperture.$

The following simple estimate can be used for beaming efficiency and determining the required aperture size. If the transmit and receive antennas are in each other's far field, one can define (from the Friis formula) a beaming efficiency as $\eta_{ij} = \frac{P_{Rj}}{P_i} = \frac{A_i A_j}{\lambda^2 R_{ij}^2}$ where the effective areas of the antennas are assumed to be equal to their geometric areas for this estimate. The distance *Rij* needs to be in the far field, and can be measured in terms of the free-space wavelength, $R_{ij} = \kappa\lambda$ (where κ is a multiplier and usually a number larger than 1000) which results in the following expression for the required aperture sizes as a function of desired beaming efficiency:

$A_i A_j = \kappa_{ij}^2 \lambda^4 \eta_{ij}$.

For the scenario from Figure 1.1, a more general beaming efficiency can be derived as follows. First, each of the 5 stations receives the following power assuming all 4 PV-powered transmitters are delivering some power to it:

$$P_{Rj} = \sum_{i=1}^{4} P_{Ti} \frac{A_j A_i}{\lambda^2 R_{ij}^2} = \frac{A_j A_i}{\lambda^4} \sum_{i=1}^{4} \frac{P_{Ti}}{\kappa_{ij}^2}$$ where j=1 to 5.

From here the beaming efficiency can be written as:

$\eta_{ij} = \frac{P_{Rj}}{\sum_{i=1}^{4} P_{Ti} / \kappa_{ij}^2} = \frac{A_i A_j}{\lambda^4}$, where the transmitted power is scaled by a unit-less number which describes the range measured in electrical distance (number of wavelengths). Alternatively, for a given beaming efficiency between any transmitter i and receiver j, the aperture sizes are estimated from:

$A_j A_i = \lambda^4 \eta_{ij}$. In the lunar surface beaming scenario, P_{Rj}=10kW, and Rij is constrained between 0.5km and 2km. The other parameters are allowed to vary and the results are plotted in Figure A1 below. In these two sample figures, the rectenna efficiency is fixed to 50% and 70%, respectively. The best reported rectenna efficiencies are around 80% (but the measurement method is not specified, so it is not clear what the number means). In the lab at CU, we have demonstrated on the order of 70-75% efficiency at low power levels, while 50% is more common for non-optimally matched rectifiers and antennas.

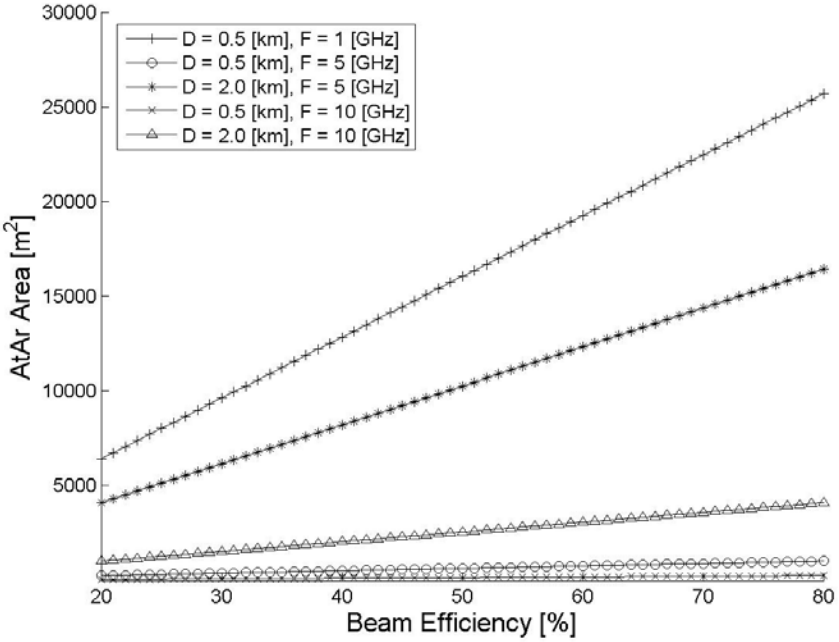

Figure A1. Example plot of product of transmit and receive apertures, in square meters, for 3 frequencies and 2 ranges (R=D=0.5 and 2km). The graph shows how the size varies as a function of beaming efficiency. Such plots were used for data summarized in Table 2.

APPENDIX B– RECTENNA ARRAY CONSIDERATIONS

A trade-off study needs to be performed to determine the optimal series-parallel configuration and physical layout for each sub-array and the converter topology for maximum system efficiency. A brief outline of such a study is given below.

We first require good understanding of the DC characteristics of the rectenna, as well as the results of constructing series/parallel combinations of rectenna elements. Similar problems have already been addressed in the field of photovoltaic cells, where many enabling technologies have matured enough to allow for progressively lower cost and higher efficiency photovoltaic power solutions to be installed in commercial facilities, as well as residential houses. As such, much research has been recently done to investigate optimal ways of harnessing and converting energy produced by solar arrays arranged in parallel/series combinations into a usable form in non-ideal environments. The goal of this part of the study is to expand our understanding of power interfaces to rectenna elements and arrays. This requires developing a more advanced and precise DC model than those used for previous research. In addition, modern power electronics and conversion techniques can be applied to the problem of rectenna arrays operating in non-uniform radiation flux conditions.

The rectenna arrays at the remote sites will necessarily have large areas (per Table 1, e.g.). The diodes in individual rectenna elements can rectify only a limited amount of power and also produce a small voltage, so series/parallel combinations of many elements must inevitably be made. With this requirement come several issues of electrical element interconnection within the array.

Figure B1 illustrates the basic constraints when connecting power-generating elements (either PV cells or rectennas) in series and parallel. A series connection will produce a higher output voltage and is needed so that the array can be more easily interfaced to an external load or power storage element. Consequently, all of the array elements must operate at the same load current. A parallel connection is needed in order to combine the current from several individual elements or strings and forces all of the elements to operate at the same voltage.

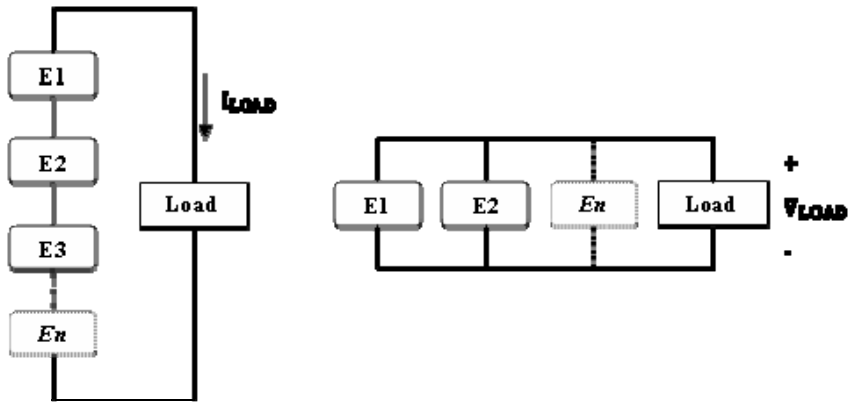

Figure B1. Series and parallel rectenna connection topologies. A series connection forces all elements to operate at the same current, while a parallel connection forces the same voltage.

Theoretically, this setup should generate *n*-times as much power as each individual element by itself if all of the elements operate under the exact same conditions in both cases. In actual real-life applications, however, this scenario is highly unlikely. Process variations in the manufacture and components of either PV cells or rectennas can lead to variations in efficiency, output

voltage and current. Moreover, it is likely that the incident power might be significantly different between elements (see Figure B1 above).

If the elements in the array being exposed to the radiation as the one in Figure 1.8 are connected randomly in series and parallel, it is likely that elements in a string will be exposed to significantly different amounts of radiation and will thus be forced to operate at a non-optimal operating point. This phenomenon is illustrated in **Figure B2**.

Figure B2(a) shows a family of I-V curves for PV cells operating at different solar flux densities. If all the elements are forced to operate at a certain string current, I_S, then two of the three elements will actual consume power instead of producing it. Specifically, the element with the highest incident power will operate at some optimal point, while the two elements with the lower incident powers will simply consume power because they are operating far away from their optimal region. A similar situation is illustrated in Figure B2(b) for several rectenna elements in series. Again, we see that only one element operates at the optimal point, while the rest either produce very little power, or even consume it.

The PV series connection problem has been studied extensively and several methods exist to prevent cells from operating in the power-consuming region. Namely, "backplane" diodes can be installed in parallel with several cells such that they become forward-biased and effectively remove cells that consume power from a string. With regards to rectenna arrays, these issues have been partially addressed in several papers based on ground-based microwave transmission experiments. These papers focused on the power that can be obtained when array elements operating at different power levels are connected in parallel and series vs. individual elements with optimal loading. All of these papers used a highly simplified DC model of the rectenna. In order to effectively design and predict the behavior of rectenna arrays, an accurate "four quadrant" model is needed which can describe the I-V characteristics of the rectenna both in power-generating mode, as well as other operating points where the rectenna might experience negative terminal voltages or currents during high-mismatch scenarios in series or parallel arrays.

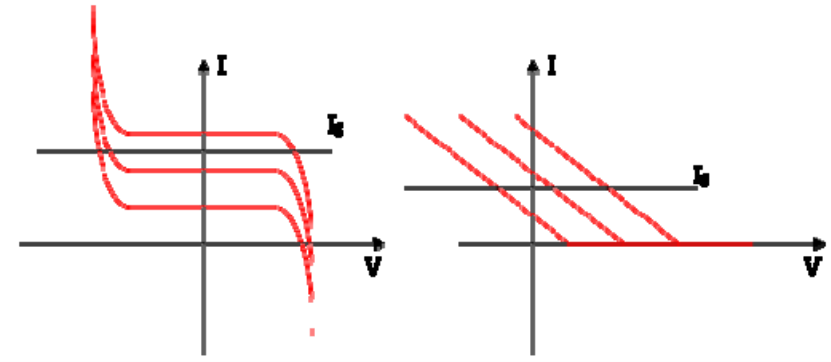

Figure B2. Comparison between solar panel (right) and rectenna (left) IV curves and series-connected operating points.

While the above study is a good start, there are still many opportunities for investigating ways for obtaining more power from the array, potentially employing similar methods to those used in PV arrays, such as backplane diodes to disconnect the elements which are consuming power. Also, the effect of series/parallel granularity – that is, how small or large the strings should be – has not been investigated. Finally, the effect of interfacing to the cells with intelligent power converters capable of either emulating the optimal load resistance or rearranging rectenna elements for maximum power extraction, as shown in **Figure B3** has not been considered at all.

The maturity of this research is relatively low compared to PV cells, however, so we need to investigate in more detail to what degree the series-connection problem exists in rectenna arrays and if similar techniques can be used to alleviate it. In order to accomplish this task, the DC characteristics of the rectenna must be understood.

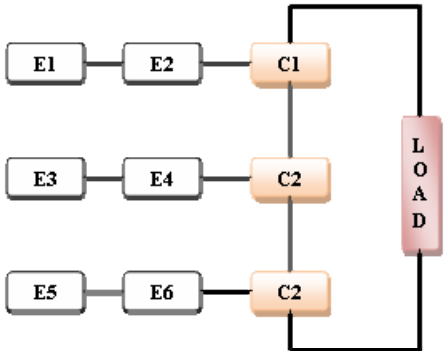

Figure B3. Rectenna elements interfaced to load through power converters.

Some previous work in has been done in developing a DC rectenna model for understanding basic ways of interfacing to the rectenna. A basic AC model consists of an AC source, an antenna series resistance, and a diode modeled as a frequency-dependent resistor in series with a capacitor. The AC signal is rectified with a diode and low-pass filtered on the output with another capacitor. This model is illustrated in **Figure B4**.

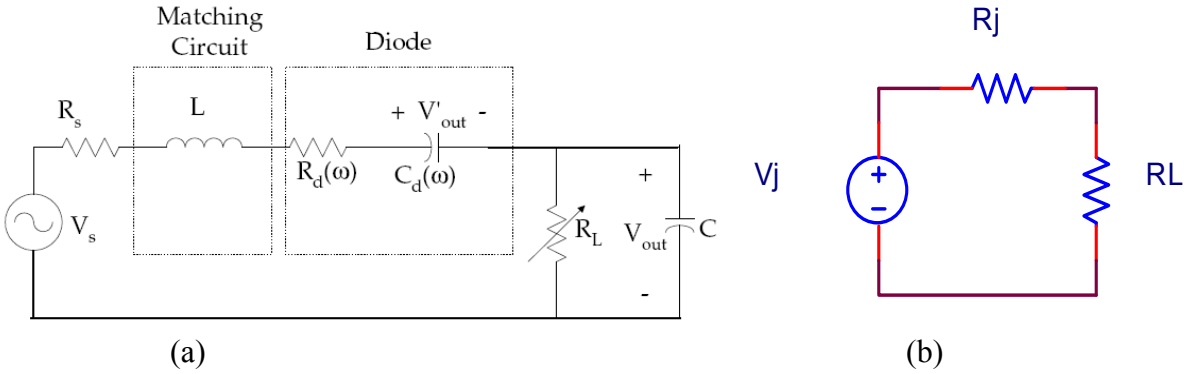

Figure B4. Simplified rectenna AC equivalent model (a) and (b) Rectenna DC equivalent model .

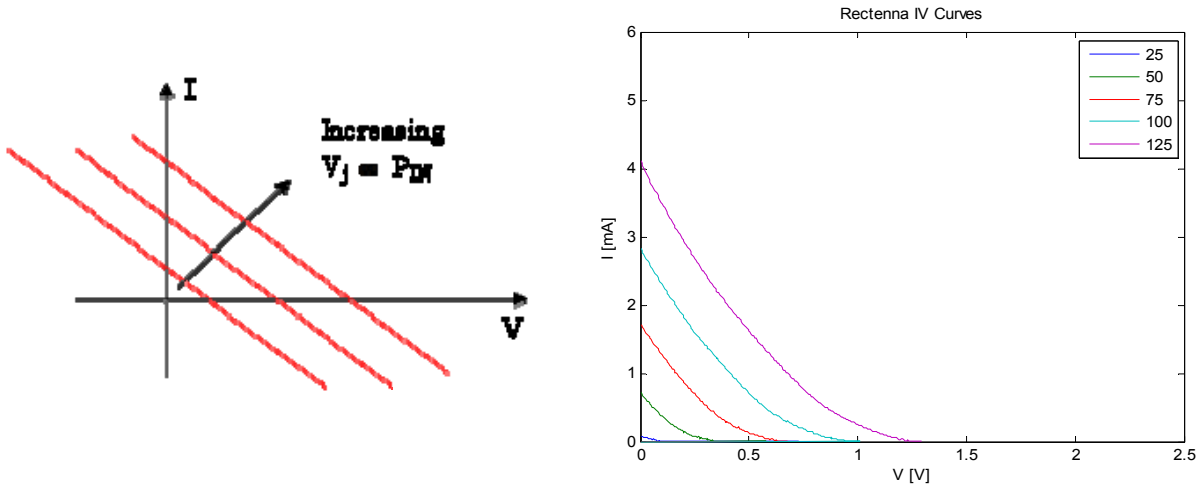

(a) (b)

Figure B5. (a) Rectenna IV curves with basic DC model. (b) Experimental rectenna IV curves for varying incident power.

The model in Figure B4(a) is generally transformed to that of Figure B4(b) to obtain a DC model. The AC source is transformed into a DC source that is proportional to the rectenna incident power. The antenna resistance and effects of the diode are lumped into a series resistance as shown. The DC model is generally used in various research papers as the basis for predicting what happens when rectennas are combined into arrays. Of course, this model gives the following equation relating the rectenna output current and voltage:

$$V = V_j + R_j \cdot I$$

where Vj and Rj are the diode junction voltage and resistance. Thus, the IV curves are as shown in **Figure B5**(a). The model seems to reasonably predict the rectenna characteristics for positive voltage and current, provided the correct values for V_j and R_j can be found. Figure B5(b) shows experimental rectenna load curves for the first quadrant of the I-V plane. The model reasonably predicts the observed curves for the first quadrant. Thus, this simple model is referred to as the "single-quadrant model".

As mentioned above, this model is used in a wide array of papers for predicting the characteristics of rectenna arrays. However, this model is only reasonably accurate for rectenna arrays composed of very similar rectennas operating at similar incident power levels – in other words, when all of the rectennas in the array are producing some net power and working in the first quadrant of the I-V plane. Of course, this is not the most general scenario, and many environments can exist which would cause partial shadowing of the array and cause some of the rectenna elements to operate out of the first quadrant. Even in radiation patterns produced by typical transmitters as shown earlier, it is possible to have elements operate out of the first quadrant. More studies need to be performed in order to precisely define the modular nature of the receiving rectenna arrays, but this short discussion points to the right direction for best efficiency.

In terms of power management at the sub-array level, a buck-boost derived topology is a likely candidate, with four operating modes: (1) buck (step-down) mode with impedance matching when the maximum power point results in a sub-array output voltage greater than 28V, (2) boost (step-up) mode with impedance matching when the maximum power point results in a subarray output voltage less than 28V, (3) pass-through mode for a direct connection from rectenna subarray to the battery when the maximum power point is within an acceptable tolerance of 28V and (4) charge control mode when battery charge limitations force operation away from the maximum power point. The power management circuit at the sub-array level efficiently accommodates a 5:1 range of power variations across the array and as function of transmitter-receiver separation and pointing accuracy.

Power monitoring functions can also be built into each power module, allowing performance data on the power transfer system to be logged. Additionally, an advantage of collecting the data at the module level is the inherent ability to detect the power beam center. This information could be used to for pointing control of the receiver or transmitter satellites or receive or transmit apertures.

To summarize, the advantages of distributed integrated harvesting modules are:

- higher overall power transfer efficiency
- graceful degradation
- approach allows for a scaled demo.

APPENDIX C – CONVENTIONAL CABLE BASELINE INFORMATION

Below are given more details for power transmission cables which were used for the efficiency and cost comparison.

National Electric Code (NEC)/Crofts American Electricians Handbook

34.5KV 40miles main line to 4 substations 10 MW

12.5 KV – step down to

7.2KV – step down to

4.16KV – step down to

120, 220, or 480V

10KW/480V = 21Amps

No.2 conductor is rated at 120A

Cables are aluminum stranded

Dry type transformers are smaller and lighter – 480V to 120V

Distance between Generation Station and Load Station is 2km one way.

Cables must go there and back = 4km or 13,123ft

Voltage drop of No.2 cable at 250DegF (121deg.C) 13,123ft is 80V.

(Temp Coef. of resistance for Al is 0.403% per Deg.C) nec

Al cable No. 2 is .26ohms/1Kft per NEC

No. 2 Duplex (Plus and Return) cable will be assumed for this application

480VDC will be assumed for this application

Load/substation requires 10KW at 480V = 21A

De-rated cable for 20A application is a 100A cable

No. 2 cable (AWG 2) is rated at 120A per NEC

According to VOLTAGE DROP Vs CABLE SIZE graph #55 of the NEC

No.2 cable will drop 45V over 7500ft at 20A. or 90V over 15000ft at 20A assumes 20C.

No. 2 cable weighs 62.3lbs/1000ft (28.3Kg/1Kft)per table 119 NEC.

No.2 cable at 4Km or **13,123ft** = 371Kg for one 10KW load station

Total Mass of Transmission Lines for 1Generation Station to 3 load stations = 1,113Kg

Four Generation Stations with three load stations each = 4,452 Kg total wire mass. Add 25% for connecting/retention hardware = 5,565Kg. Add another 25% for packaging and deployment hardware = 7,000Kg Total cable system mass.

A step down transformer will be required at the load station to go from 400V to 120V or 28V. Estimated Mass – 10KW, Converter = 100Kg each. Need 5 converters for a total **500Kg.**

Total Launched Mass of Conventional Transmission Line System = 7,500kg

Preliminary Calculation For Cable Efficiency (Loss)

- $V_{drop} = I_{load} \text{ x } R_{cable}$
- $I_{load} = 21A$
- $R_{cable} = 0.26ohms/1000ft$, for 13,123ft = 3.41Ohms
- $V_{drop} = 21A \text{ X } 3.41Ohms = 72V$
- $V_{drop} = 72V$ Cable Drop
- Add 10% for Interconnections = 79.2V, round up to 80V.
- 20degC is the baseline.
- Lunar surface temp is 121degC
- This gives a 101deg C differential
- No.2 Al cable has a resistive temp. coeffient. of 0.403%per deg C.
- 101degC * .403% = 40.7%
- Voltage drop will be increased by 40.7% over the 20degC baseline
- Therefore:
- 80Vdrop X 1.407 = 112.56V round up to 113Vdrop
- 113V Total Voltage Drop between Solar Gen. Station and Load Station at 21 Amps and 121degC
- 480V – 113V = 367Vdc at the Load Station.
- 367Vdc will be down converted to 120Vdc for user loads.

APPENDIX D – COST AND MASS SUMMARY

Description	Quantity			Per Unit COST	Total COST	
Mass Category / Power Category	**EDU (#)**	**Per Unit CBE (kg)**	**Total (kg)**			
PMAD					**GFE**	
Transmitters and Rectennas		**4193.04**			**TOTAL COST**	**$ 12,693,627**
Transmitting Antenna Emitters (5m x 5m planar array)	**1**		**612.32**	**$ 70,082**	**$ 1,258,333**	**$ 5,033,331**
Antenna Elements	16666	0.01	166.66	14	233324	
VCOs (voltage controlled oscillators)	16666	0.00	16.67	12	199992	
Several Gain Blocks	50000	0.00	100.00	2	100000	
Driver Amp	16666	0.00	33.33	10	166660	
GaN device	16666	0.01	166.66	13	208325	
Feed Line to N elements (64)	1	0.00	0.00	10	10	
Harness	1	4.00	4.00	22	22	
Bias Distribution Network	1		0.00	0	0	
FITS	5	0.75	125.00	70000	350000	
Rectenna Elements (Load Facility = 21m x 21m)	**1**		**348.75**	**72481**	**1532059**	**7660296**
Antenna Elements	1260	0.01	12.60	14	17640	
Schottky diodes	1260	0.00	1.26	0	252	
Power Management Circuit	21	0.05	1.05	2000	42000	
Converters	21	0.05	1.05	50	1050	
Microcontroller	21	0.05	1.05	35	735	
Harness	1	0.99	0.99	382	382	
Bias Distribution Network	1		0.00	0	0	
FITS	21	0.75	330.75	70000	1470000	
Transmitting Mast	**1**					
Transmitting Mast - 20 m Tall	4	100.00	**400.00**	100000	400000	**400000**